



저작자표시-비영리-동일조건변경허락 2.0 대한민국

이용자는 아래의 조건을 따르는 경우에 한하여 자유롭게

- 이 저작물을 복제, 배포, 전송, 전시, 공연 및 방송할 수 있습니다.
- 이차적 저작물을 작성할 수 있습니다.

다음과 같은 조건을 따라야 합니다:



저작자표시. 귀하는 원저작자를 표시하여야 합니다.



비영리. 귀하는 이 저작물을 영리 목적으로 이용할 수 없습니다.



동일조건변경허락. 귀하가 이 저작물을 개작, 변형 또는 가공했을 경우에는, 이 저작물과 동일한 이용허락조건하에서만 배포할 수 있습니다.

- 귀하는, 이 저작물의 재이용이나 배포의 경우, 이 저작물에 적용된 이용허락조건을 명확하게 나타내어야 합니다.
- 저작권자로부터 별도의 허가를 받으면 이러한 조건들은 적용되지 않습니다.

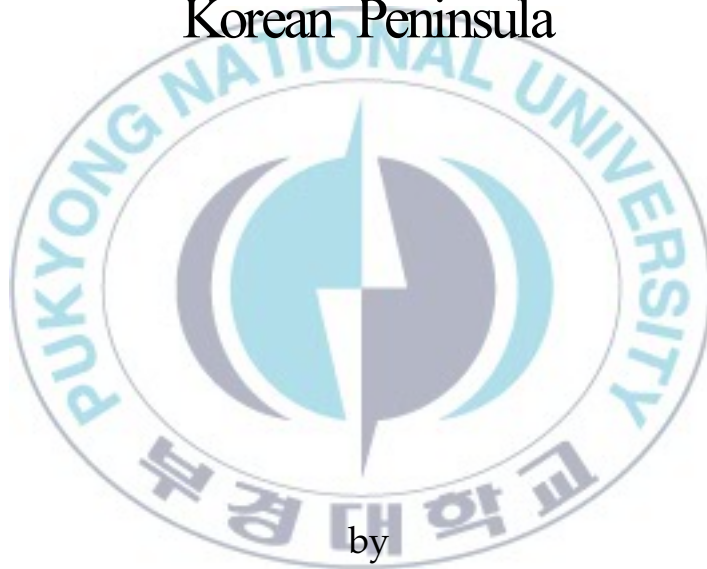
저작권법에 따른 이용자의 권리는 위의 내용에 의하여 영향을 받지 않습니다.

이것은 [이용허락규약\(Legal Code\)](#)을 이해하기 쉽게 요약한 것입니다.

[Disclaimer](#)

Thesis for Degree of Master of Engineering

Development of Snowfall Retrieval
Algorithm by Combining Data from
CloudSat, NOAA, AQUA Satellites for the
Korean Peninsula



by

Na Ri Kim

Department of Spatial Information Engineering

The Graduate School

Pukyong National University

February 2012

Development of Snowfall Retrieval Algorithm by
Combining Data from CloudSat, NOAA, AQUA
Satellites for the Korean Peninsula

(CloudSat, NOAA, AQUA 위성자료를
결합한 한반도 지역의 강설 추정
알고리즘 개발)

Advisor: Prof. Young Seup Kim

by

Na Ri Kim

A thesis submitted in partial fulfillment of the requirements
for the degree of

Master of Engineering

in Department of Spatial Information Engineering,
The Graduate School, Pukyong National University

February 2012

Development of Snowfall Retrieval Algorithm by Combining Data
from CloudSat, NOAA, AQUA satellites for the Korean Peninsula

A thesis
by
Na Ri Kim

Approved by:



(Chairman) Hong Joo Yoon



(Member) Kyung Soo Han

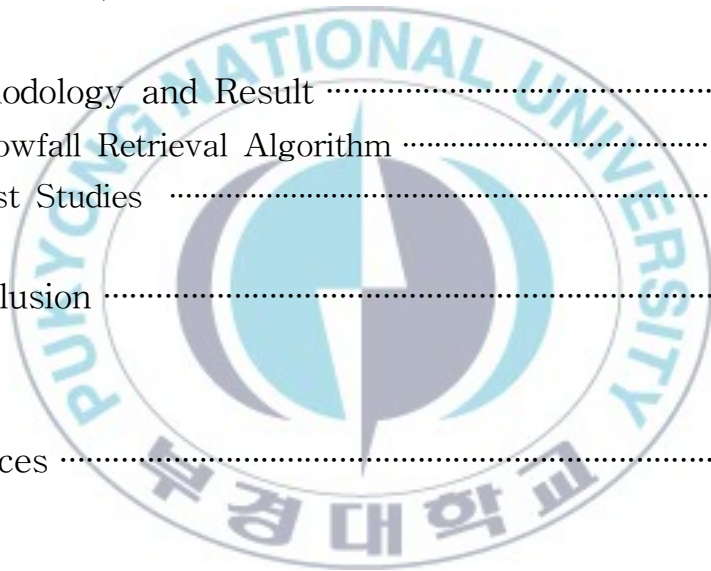


(Member) Young Seup Kim

February 25, 2012

Contents

1. Introduction	1
2. Data	4
2.1. CloudSat Cloud Profiling Radar data	6
2.2. AQUA/AMSR-E data	12
2.3. NOAA-18/MHS data	14
3. Methodology and Result	16
3.1. Snowfall Retrieval Algorithm	16
3.2. Cast Studies	26
4. Conclusion	32
References	34



List of Figures

Fig. 2. 1. Study area	5
Fig. 2. 2. Sample images for heavy snowfall by CloudSat in the Korean peninsula	11
Fig. 3. 1. Flow chart of snowfall retrieval with combining CloudSat, AMSR-E, and MHS	16
Fig. 3. 2. Reflectivity scatter diagrams for CloudSat and CloudSat/MHS combination, (a) January, and (b) February, 2008	24
Fig. 3. 3. Reflectivity scatter diagrams for CloudSat and CloudSat/AMSR-E combination, (a) January, and (b) February, 2008	25
Fig. 3. 4. Images of CloudSat and MHS channels on Feb. 3, 2008	28
Fig. 3. 5. Images of CloudSat and AMSR-E channels on Feb. 3, 2008	29
Fig. 3. 6. Snowfall cloud image comparison for instantaneous profile by CloudSat and horizontal distribution by CloudSat/MHS retrieval equation, February 3, 2008	30
Fig. 3. 7. Snowfall cloud image comparison for instantaneous profile by CloudSat and horizontal distribution by CloudSat/AMSR-E retrieval equation, February 3, 2008	31

List of Tables

Table. 2. 1. System characteristics of CloudSat CPR	8
Table. 2. 2. CloudSat standard data products	9
Table. 2. 3. Description of CloudSat cloud mask values	10
Table. 2. 4. Specification of AMSR-E onboard AQUA	13
Table. 2. 5. Specification of MHS onboard NOAA-18	15
Table 3. 1. Mode values of Clear Sky for MHS channels in February 2008	20
Table 3. 2. Mode values of Clear Sky for AMSR-E channels in February 2008	20
Table 3. 3. Regression coefficients $\alpha_1 - \alpha_7, \beta$ derived from CloudSat/MHS algorithm in Jan. and Feb. 2008	23
Table 3. 4. Regression coefficients $\alpha_1 - \alpha_4, \beta$ derived from CloudSat/AMSR-E algorithm in Jan. and Feb. 2008	23

CloudSat, NOAA, AQUA 위성 자료를 결합한
한반도 지역의 강설추정 알고리즘 개발

김 나 리

부 경 대 학 교 대 학 원 위 성 정 보 과 학 과

요 약

최근 기후변화로 인해 강설강도가 점점 강해지고 폭설의 사례가 급증함으로써 위성파 레이더를 이용한 강설추정에 관한 연구가 활발히 진행되고 있다. 기존의 연구들은 일반적으로 수동 마이크로파 센서를 이용하여 강설을 추정하는 기법을 채택하고 있다. 그러나 수동 마이크로파 센서만을 이용한 강설 추정은 대기의 연직 구조 파악이 힘들기 때문에 정확한 강설량을 추정하는 데에 한계가 있다. CloudSat의 구름 레이더는 강설의 연직 프로파일에 대한 가치있는 정보를 제공하므로, 수동 마이크로파 센서와의 결합을 통해 새로운 강설 추정 알고리즘을 제시할 수 있다.

본 연구에서는 능동 마이크로파 센서인 CloudSat의 Cloud Profiling Radar와 수동 마이크로파 센서인 NOAA/MHS와 AQUA/AMSR-E 자료를 각각 결합하여 한반도에 적합한 강설 추정 알고리즘을 개발하고, 그 활용 가능성을 조사하였다. 강설에 대한 특징을 보다 자세히 분석하기 위해 각각의 자료에 대한 주성분 분석을 수행하였고, 산출된 값들을 결합하여 강설 추정 알고리즘을 개발하였다. 최종적으로 개발된 알고리즘에 수동마이크로파 자료만을 이용하여 Z' 값을 산출하였고, CloudSat의 Z' 값에 대한 상관관계를 조사하였다. 이를 통해 강설에 대한 관측 가능성과 그 활용성을 확인할 수 있었다. CloudSat 통과시의 실제 관측 영상과 두 센서의 결합 알고리즘에 의한 영상을 비교하여, 알고리즘의 활용 가능성이 확인되었으며 육상에 대해서는 추가적인 연구가 필요한 것으로 판단된다.

1. Introduction

Snowfall is a very important component in the climate system and plays a key role in the hydrological cycle. Snowfall of Korean winter season is below 10% of annual precipitation, but it is an important factor for the water resources of spring season and decrease of forest fire. However, the heavy snowfall cases increasing rapidly by the climate change. The number of snowfall days is similar to every year, but snowfall strength is increasingly severe. The snowfall disaster affect from occurrence time, and it affect a variety of environment and society system. Because it piled up during a certain period after snowfall occurring (Robinson, 1989; Schmidlin, 1993). Thus, we effort into retrieving of snowfall and checking the whether or not snowfall is true for decreasing damage by heavy snowfall.

Methods are to monitor the snowfall that ground observation system such as snowfall gauges, AWS and radar have been used, but these monitoring systems are sparsely distributed and have been an effect on the land. So such monitoring systems are difficult to snowfall retrieval, because it was not represented for the homogeneous distribution of snowfall area, and the inadequacy of data has arisen (Park, 2000).

Snowfall retrieval method using the satellite data is becoming the popular method because it could get easily a variety of

channel data and can monitoring and measurements for snowfall from wide area without influence of land(Kim and Park, 2002). Choi and Shin(1990) revealed the extrapolability for cloud depth and possibility of perceptible water retrieval using the brightness temperature of GMS satellite. Lee et al(1994) also studied for the method of precipitation estimation by measurements of GMS(VIS, IR) and Gwanak radar, and many researchers were studied for snowfall retrieval methods using brightness temperature of cloud(Seo et al, 1994; Lee et al, 1994). However, the method using the VIS and IR of satellite is indirect. Satellites can detect the cloud brightness temperature and cloud top temperature, but cannot detect the particles. So unique limitation is existent. Gruber(1973) pointed out that the method using VIS and IR inappropriate to analogize with detailed section of convective activity. Atlas(1982) also pointed out the riskiness that method using VIS and IR from a geostationary satellite applied for estimating precipitation of each storm. However, the microwave can relatively estimate snowfall rate, because it can penetrate the cloud and provide the height and attribute data of cloud. Therefore, it is mostly used about snowfall retrieval studies.

Many international researchers show high interest for development of snowfall retrieval algorithm using passive microwave sensors. Limin Zhao and Fuzhong Weng(2002) developed the algorithm estimated the Ice Water Path and

particle size using 89, 150 GHz channels of AMSU. Cezar Kongoli et al(2003) was improved the existing rainfall algorithm by AMSU data, and then it applied for snowfall detection. Haddad and Park(2009) derived the algorithm by combining measurements from TRMM/PR sensor and radiometer data. Studies of development of snowfall retrieval algorithm for using the passive microwave sensor are steadily proceeding. However, snowfall retrieval from the passive microwave sensor has limit to accurate estimation, because it is difficult to understand for vertical profile of atmosphere.

In this study, we develop snowfall retrieval algorithm by combining measurements from CloudSat cloud radar as an active microwave sensor, Aqua/AMSR-E and NOAA-18/MHS, and investigate an application possibility from case studies.

2. DATA

The study area is the Korean Peninsula bounded by 30 ~ 45°N and 120 ~ 135°E(Figure 2.1.). The snowfall was estimated over the study period from December to February in winter season of Korea. This study used CloudSat Cloud Profiling Radar (CPR) products (2B-GEOPROF), MHS sensor data and AMSR-E sensor data. CloudSat CPR products(2B-GOEPROF) was provided in the CloudSat Data Processing Cetner (<http://www.cloudsat.cira.colostate.edu>), AMSR-E and MHS data was obtained in FTP directory and NOAA web site, respectively. We used the data processing using program such as IDL 6.0 and Matlab R2008b.

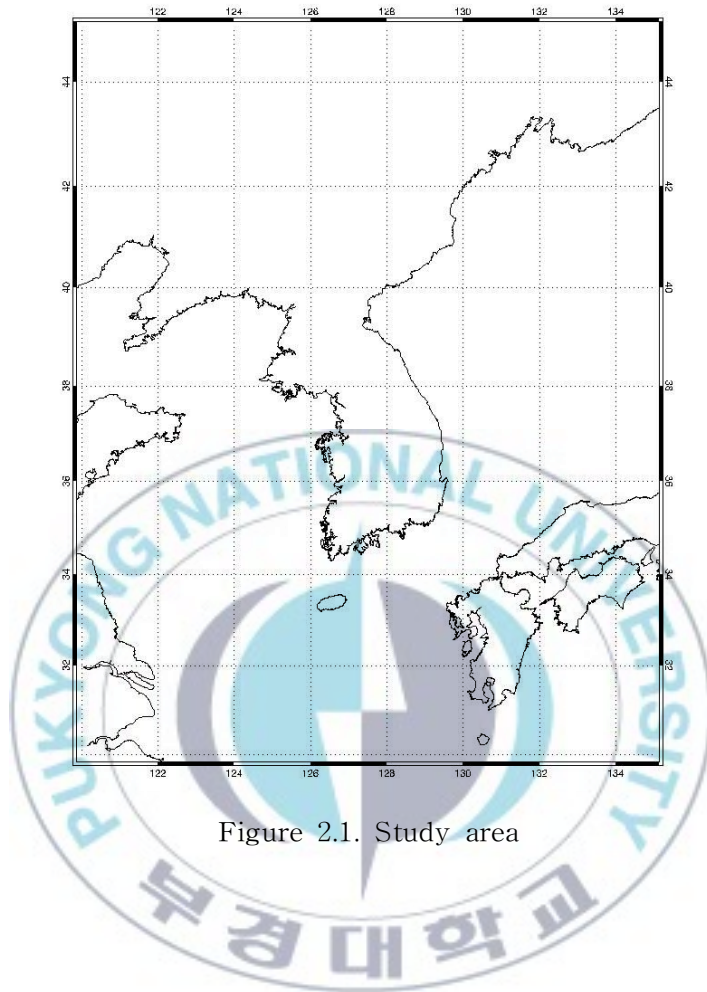


Figure 2.1. Study area

2.1. CloudSat Cloud Profiling Radar Data

CloudSat was launched in April 2006, and a NASA Earth Sciences Systems Pathfinder (ESSP) mission. The main purpose of CloudSat mission is to measure the vertical structure of clouds and will simultaneously observe cloud and precipitation(NASA ESSPM, 2008). It is a polar-orbiting satellite within A-Train constellation, included Aqua, AURA, CALIPSO and so on. CloudSat carries the Cloud Profiling Radar as an active microwave sensor. CPR is a 94-GHz nadir-looking radar and was developed jointly by NASA/JPL and the Canadian Space Agency(CSA). The vertical and horizontal resolution of CPR are 500 m and 1.4×1.7 km, respectively, and it has a sensitivity of -29 dBZ, such that CloudSat is able to detect most, but not all, tropospheric clouds(Sassen and Wang, 2008). It is very sensitive for the ice particles and, is very useful for understanding of cloud characterization, because it also provides valuable information for the vertical profiles of snowfall(Matrosov et al, 2008)(Table 2.1).

CPR provides level 1 and 2 products and Table 2.2 was represented descriptions for these products. The design of CPR is driven by its scientific objectives. The sensitivity defined by a minimum detectable reflectivity factor of -30 dBZ, and a calibration accuracy of 1.5 dB(Kim et al, 2011). In this study, we

used 2B-GEOPROF products, applied the cloud mask and radar reflectivity(Figure 2.2). The information about cloud mask flag showed Table 2.3. In order to get the snowfall data, we build the database in case that there are cloud mask flags and reflectivity values more than 3 and - 5 dBZ from land surface.



Table 2.1 System characteristics of CloudSat CPR

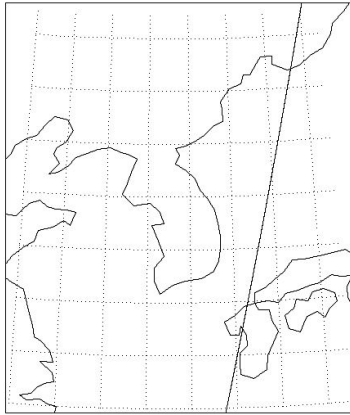
Nominal Frequency	94 GHz
Pulse Width	3.63 μ sec
PRF	4300 Hz
Minimum Detectble Z	< -29 dBZ
Data Window	0 - 25 km
Antenna Size	1.85 m
Dynamic Range	70 dB
Integration Time	0.16 sec
Nadir Angle	0.16°
Vertical Resolution	500 m
Cross-Track Resolution	1.4 km
Along-Track Resolution	1.7 km
Data Rate	20 kbps

Table 2.2 CloudSat standard data products

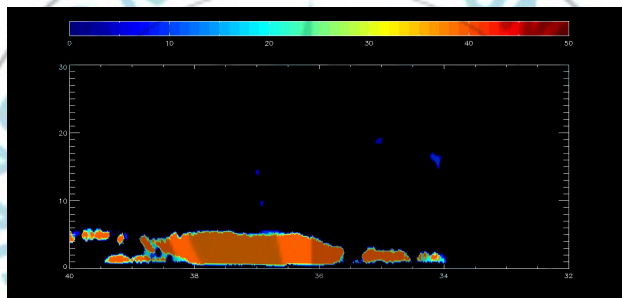
Product	Description
1B-CPR and 1B-CPR-FL	Radar Backscatter Profiles
2B-GEOPROF	Cloud Geometrical Profile
2B-CLDCLASS	Cloud Classification
2B-CWC-RO	Combined Water Content - Radar Only
2B-TAU-OFF-N	Cloud Optical Depth - Off Nadir
2B-CWC-RVOD	Combined Water Content - Radar + Vis. Optical Depth
2B-FLXHR	Fluxes and Heating Rates
2B-GEOPROF-Lidar	Cloud Geometrical Profile from CPR and CALIPSO Lidar
2B-CLDCLASS-Lidar	Cloud Classification from CPR and CALIPSO Lidar

Table 2.3 Description of CloudSat cloud mask values (NASA ESSPM, 2007)

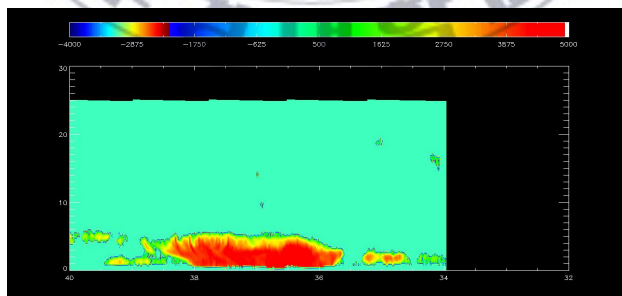
Mask Value	Meaning
-9	Bad or missing radar data
5	Significant return power but likely surface clutter
6 ~ 10	Very weak echo (detected using along-track averaging)
20	Weak echo (detection may be artifact of spatial correlation)
30	Good echo
40	Strong echo



(a) Orbit of CloudSat



(b) Cloud Mask



(c) Radar Reflectivity

Figure 2.2. Sample image for heavy snowfall by CloudSat in the Korean peninsula

2.2. AQUA/AMSR-E Data

Advanced Microwave Scanning Radiometer for the Earth Observing System(AMSR-E) is a passive microwave radiometer on board AQUA satellite since May 2002. It has six-frequency and twelve-channels, with 6.925, 10.75, 18.7, 23.8, 36.5, 89.0-GHz. Each of channels is polarized and all of the channels detect the brightness temperature emitted from the earth. It provides the global dataset for a variety of weather and climate studies, and useful for measuring meteorological variables(such as all-weather sea surface temperature, sea ice extent, oceanic integrated cloud water and water vapor, precipitation, soil wetness, snow water content) in cloudy regions of atmosphere(Lobl et al, 2009). Aqua/AMSR-E, A-Train satellite in common with Cloudsat, has nearly same orbit with CloudSat. These two satellites collect data almost simultaneously, because CloudSat lags behind the Aqua satellite by approximately 90 seconds. Table 2.4 is represented the specification of Aqua/AMSR-E sensor.

Table 2.4 Specification of AMSR-E onboard AQUA

Center Frequencies (GHz)	6.9	10.7	18.7	23.8	36.5	89.0
Mean Spatial Resolution (km×km)	56	38	21	24	12	5.4
IFOV (km×km)	75×43	51×29	27×16	32×18	14×8	6×4
Sampling Rate (km×km)	10×10	10×10	10×10	10×10	10×10	5×5
Sensitivity (K)	0.3	0.7	0.7	0.7	0.6	1.2
Integration Time (msec)	2.6	2.6	2.6	2.6	2.6	1.3
Main Beam Efficiency (%)	95.3	95.0	96.4	96.4	95.3	96.0
Beamwidth (degrees)	2.2	1.4	0.9	0.9	0.4	0.18
Orbit (km)	705 (sunsynchronous, ±82 latitude)					
Repeat cycle (day)	16					
Swath (km)	1450					
Data size / Scene (MB)	21 (including all channels & levels to L1B)					

2.3. NOAA-18/MHS Data

Microwave Humidity Sounder(MHS) is a passive microwave sensor on board the National Oceanic and Atmospheric Administration(NOAA) polar-orbiting platforms, and is a revised version of AMSU-B. It has five channels with 89, 157, 183.3±1, 183.3±3 and 190 GHz, and its footprint is 16 × 16 km at nadir. The antenna beamwidth is a constant 1.1 degrees at the half-power point at each channel frequency(Kim et al, 2011).

MHS provides products such as rain rate, ice water path, snow cover, snow water equivalent and so on. Since MHS has a wider swath than SSM/I and TMI, it observes around East Asia at least twice a day. It can also utilize high frequency ranges for scattering characteristics of snowfall cloud and apply the land and ocean simultaneously. Table 2.5 is represented the specification of NOAA-18/MHS sensor.

Table 2.5 Specification of MHS onboard NOAA-18

Frequencies (GHz)	89.0	157.0	183±1	183±3	190
Polarization	vertical	vertical	horizontal	horizontal	vertical
Sensitivity (K)	0.22	0.34	0.51	0.40	0.46
Beamwidth (MHz)	2800	2800	2×500	2×1000	2200
Swath (km)	1650 km				
Spatial resolution	17 km horizontal at nadir				
Field of View	± 49.5 degrees cross-track				
IFOV	1.1 degrees circular				

3. METHODOLOGY AND RESULT

3.1. Snowfall Retrieval Algorithm

Figure 3.1. is a flow chart of snowfall retrieval with combining CloudSat and AMSR-E or MHS for this study.

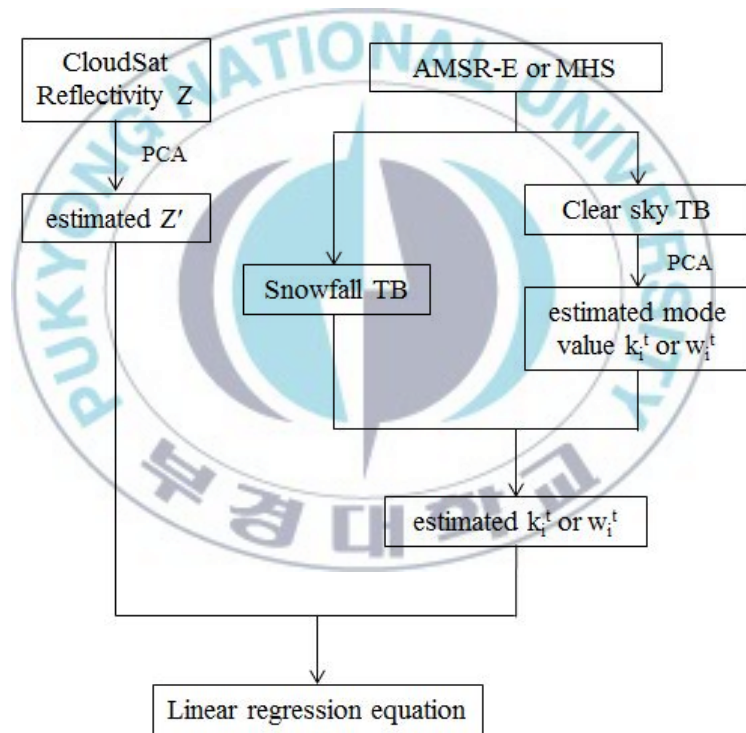


Figure 3.1. Flow chart of snowfall retrieval with combining CloudSat, AMSR-E, and MHS

We used reflectivity of vertical 20 observed from surface by CloudSat and brightness temperature of AMSR-E 9 channels and MHS 5 channels to snowfall retrieval in January and February 2008.

These data has errors for differences of observing location and resolution between CloudSat-CPR and AMSR-E, and CloudSat-CPR and MHS. So we collected data that spatial difference of latitude and longitude between two satellites was less than 1 degree. Then, temporal difference between CloudSat and MHS was within 5 minutes, but it between CloudSat and AMSR-E was not considering because temporal difference is approximately 90 seconds. Spatial resolution fitted by averaging values of CloudSat radar which have relatively good resolution(1.4×1.7 km).

Principle Component Analysis(PCA) is the main analysis method used in this study. Principle Components Analysis that information of multi-dimensional data is abbreviated to 2- or 3-dimensional data minimize the loss of data information, it make visually understanding that there is observation targets in any position. To achieve this, we should search the axis maximized dispersion. If data is analyzed from which, information each of characteristics is easily found. Therefore, we perform the principle components analysis to analyze snowfall characteristics in detail.

Based on database for January and February 2008, AMSR-E and MHS data was classified as clear sky data and snowfall data. Brightness temperature calculated each of AMSR-E and MHS channels is influenced by land and atmosphere, simultaneously. In particular, low frequency microwave channels is affected by land than atmosphere, so it very important to remove influences of land. Removing them, we perform the principle components analysis for clear sky data of AMSR-E and MHS. As a result, mode 1 and 2 of AMSR-E and mode 1 of MHS represented influence of land was discarded, and then other eigenvector was used. Table 3.1 and Table 3.2 was represented eigenvector for AMSR-E and MHS. Eigenvector discarded influence of land and brightness temperature each of channels for snowfall was inputted into following equation, and then we got the channels value weighted snowfall characteristics.

$$k_i^t T = a_i T_1 + b_i T_2 + c_i T_3 + d_i T_4 + e_i T_5 + f_i T_6 + g_i T_7 + h_i T_8 + i_i T_9 \quad (1)$$

where

$k_i^t T$ = Weighted AMSR-E channels value by snowfall characteristic (i=3~9)

$T_1 \sim T_9$ = Brightness temperature for AMSR-E 9 channels

$a_i \sim i_i$ = Eigenvector of AMSR-E channels (i=3~9)

$$w_i^t T = a_i T_1 + b_i T_2 + c_i T_3 + d_i T_4 + e_i T_5 \quad (2)$$

where

$w_i^t T$ = Weighted MHS channels value by snowfall characteristic (i=2~5)

$T_1 \sim T_5$ = Brightness temperature for MHS 5 channels

$a_i \sim e_i$ = Eigenvector of AMSR-E channels(i=2~5)

Through equations, $k_i^t T$ and $w_i^t T$ weighted channels value by snowfall characteristic was calculated.

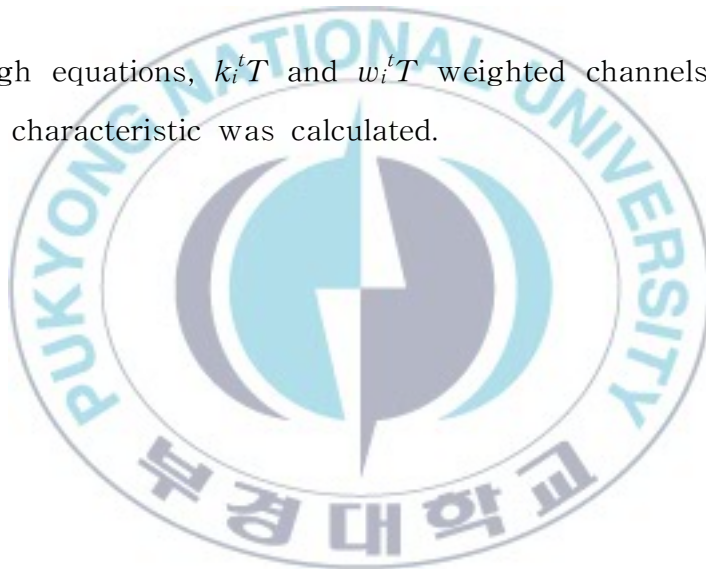


Table 3.1 Mode values of Clear Sky for MHS Channels in February 2008

	a_i	b_i	c_i	d_i	e_i
mode2	-0.408	0.412	0.203	0.352	0.703
mode3	0.289	-0.491	0.632	0.523	0.118
mode4	0.213	-0.490	-0.652	0.198	-0.499
mode5	-0.108	0.253	-0.364	0.749	-0.479

Table 3.2 Mode values of Clear Sky for MHS Channels in February 2008

	a_i	b_i	c_i	d_i	e_i	f_i	g_i	h_i	i_i
mode3	0.598	-0.222	-0.382	-0.459	-0.206	0.004	-0.232	0.374	0.015
mode4	0.239	-0.505	0.465	-0.108	-0.023	0.328	-0.082	-0.390	-0.441
mode5	-0.190	0.439	0.325	-0.050	-0.534	0.120	-0.393	0.310	-0.335
mode6	-0.171	0.365	-0.351	-0.445	0.218	0.661	0.175	-0.184	-0.207
mode7	-0.046	-0.016	-0.068	0.140	0.687	-0.142	-0.375	0.333	-0.480
mode8	-0.084	0.123	0.426	-0.582	0.305	-0.179	-0.347	-0.135	0.441
mode9	0.008	-0.048	-0.237	0.391	-0.009	0.429	-0.650	-0.231	0.359

Next, we perform the principle components analysis for CloudSat reflectivity data. In order to extract components about snowfall, we performed principle components analysis using vertical 20 reflectivity from surface. As a result, mode 1 value is represented the snowfall effect very well, and coordinative Z' which is weighted reflectivity each of levels was calculated using mode 1 value.

In order to derive suitable regression equation for heavy snowfall cases, Z' value for CloudSat was categorized into five according to size, and then we perform the multiple regression analysis using weighted value of AMSR-E and CloudSat, MHS and CloudSat for each of categories.

- A : $Z' < \bar{x}$
 B : $\bar{x} < Z' < \bar{x} + 0.5s_x$
 C : $\bar{x} + 0.5s_x < Z' < \bar{x} + 1.0s_x$
 D : $\bar{x} + 1.0s_x < Z' < \bar{x} + 1.5s_x$
 E : $Z' > \bar{x} + 1.5s_x$

By the analysis, the best result is values of regression equation for E category. The linear regression equation for AMSR-E and MHS is equation (1) and equation (2), regression coefficients were represented Table 3.1 and Table 3.2.

$$Z' = \alpha_1 k_3^t T + \alpha_2 k_4^t T + \alpha_3 k_5^t T + \alpha_4 k_6^t T + \alpha_5 k_7^t T + \alpha_6 k_8^t T + \alpha_7 k_9^t T + \beta \quad (3)$$

where

$\alpha_1 \sim \alpha_7, \beta$ = regression coefficients for AMSR-E

$$Z' = \alpha_1 k_2^t T + \alpha_2 k_3^t T + \alpha_3 k_4^t T + \alpha_4 k_5^t T + \beta \quad (4)$$

where

$\alpha_1 \sim \alpha_4, \beta$ = regression coefficients for MHS

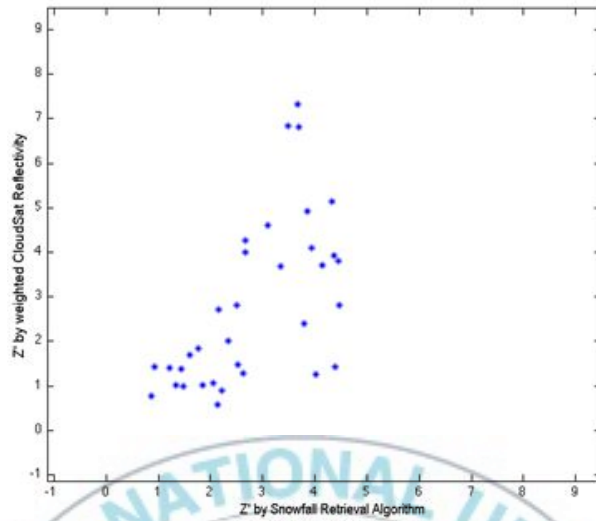
We estimated Z' at derived snowfall retrieval algorithm using only passive microwave sensor data. The correlation analysis was performed by Z' from CloudSat and combined algorithm, and Figure 3.2 and Figure 3.3 are represented results. Correlation coefficient for algorithm of AMSR-E and CloudSat is 0.66 in January and 0.60 in February, 2008, and RMSE is 2.67 and 2.36, respectively. Correlation coefficient for algorithm of MHS and CloudSat is 0.67 in January and 0.596 in February, 2008, and RMSE is 2.27 and 1.92, respectively.

Table 3.3 Regression coefficients $\alpha_1 - \alpha_7$, β derived from CloudSat/MHS algorithm in January and February 2008

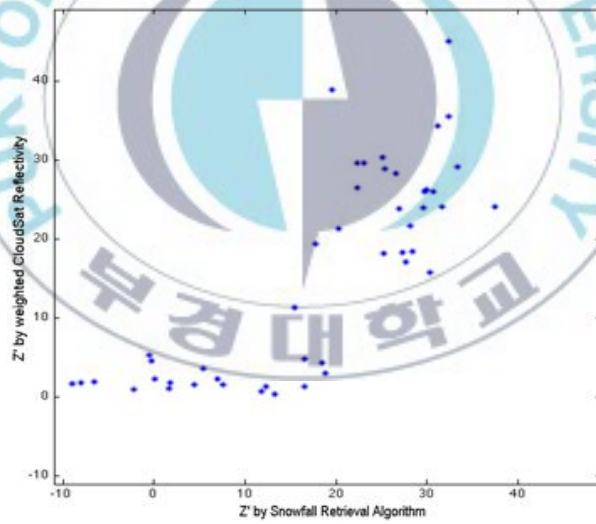
	α_1	α_2	α_3	α_4	β
Jan 2008	0.04	-0.216	-0.16	-0.17	42.94
Feb 2008	-2.42	-0.767	-4.68	-0.78	750.80

Table 3.4 Regression coefficients $\alpha_1 - \alpha_7$, β derived from CloudSat/AMSR-E algorithm in January and February 2008

	α_1	α_2	α_3	α_4	α_4	α_4	α_4	β
Jan 2008	0.73	0.20	-0.21	0.004	0.09	-0.06	0.004	28.02
Feb 2008	0.14	0.20	-0.79	0.16	0.02	-0.10	0.04	-33.55

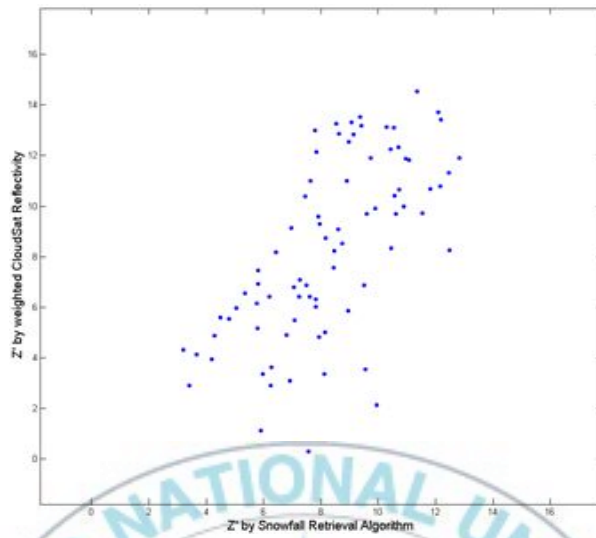


(a) Jan, 2008

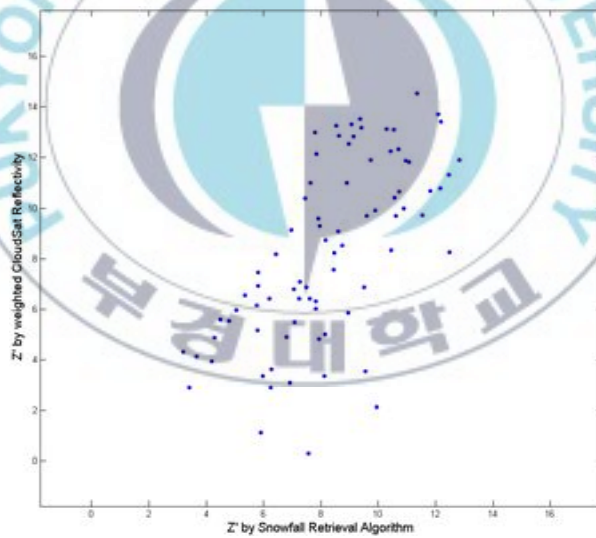


(b) Feb, 2008

Figure 3.2. Reflectivity scatter diagrams for CloudSat and CloudSat/MHS combination, (a) January, and (b) February, 2008



(a) Jan, 2008



(b) Feb, 2008

Figure 3.3. Reflectivity scatter diagrams for CloudSat and CloudSat/AMSR-E combination, (a) January, and (b) February, 2008

3.2. Case Study

We perform case studies in Feb. 3, 2008, using developed snowfall retrieval algorithm in this study.

Figure 3.4 was represented images for brightness temperature of MHS channels(89.0, 157.0, 183±1, 183±3, 190.0 GHz) in February 3, 2008. In images of 89.0 and 157 GHz channels, high brightness temperature was represented on land, and image of 183±1 GHz channel was generally represented low values except for some parts of the southern sea, and images of 183±3 and 190 GHz channels generally showed high brightness temperature except some part of Russia. Therefore, it was difficult to obtain the accurate snowfall signals through each of channels images.

Figure 3.5 was represented images for vertical polarized brightness temperature of AMSR-E channels(10.65, 18.7, 23.8, 36.5, 89.0 GHz) in same day. Since low frequency channels such as 10.65 and 18.7 GHz was seriously influenced by land effects, brightness temperature in land was high values and in ocean was low values. Therefore, boundary between land and ocean was clearly divided. On the other hand, high frequency channels such as 23.8, 36.5, and 89.0 generally show the volume scattering for snowfall ice particle in ocean, but were difficult to search accurate snowfall signals.

Figure 3.6 and Figure 3.7 are to represent reflectivity images

by CloudSat and images applied algorithm of MHS and CloudSat, and AMSR-E and CloudSat. Through these images, A~B and C~D areas which is the East Sea including Ullengdo was represented that reflectivity value is 6~14 and 30~70, respectively, and we confirmed higher Z' value than around area. Then, we know to exist snowfall cloud that has more 10 dBZ than around area, through CloudSat reflectivity images. The developed snowfall retrieval algorithm in this study was confirmed to calculate accurate result relatively, because snowfall of approximately 86.5 cm was fell in Ullengdo by Annual Climatological Report of Korea Meteorological Administration in 2008.



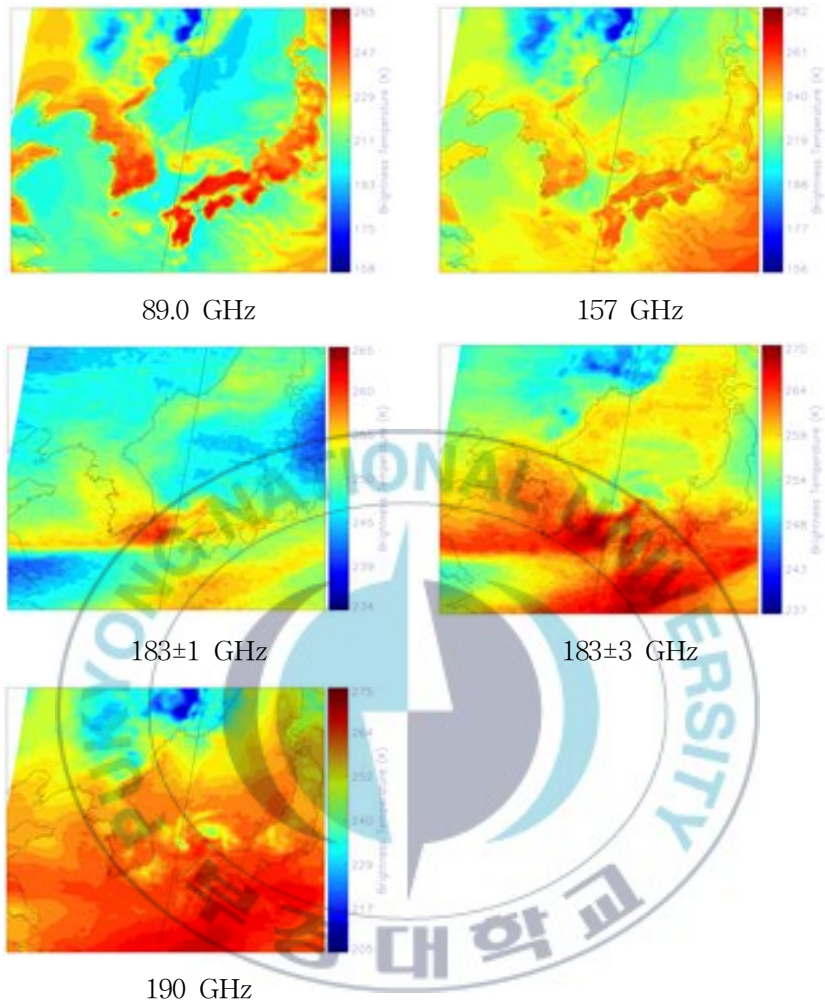


Figure 3.4. Images of CloudSat and MHS channels on Feb. 3, 2008

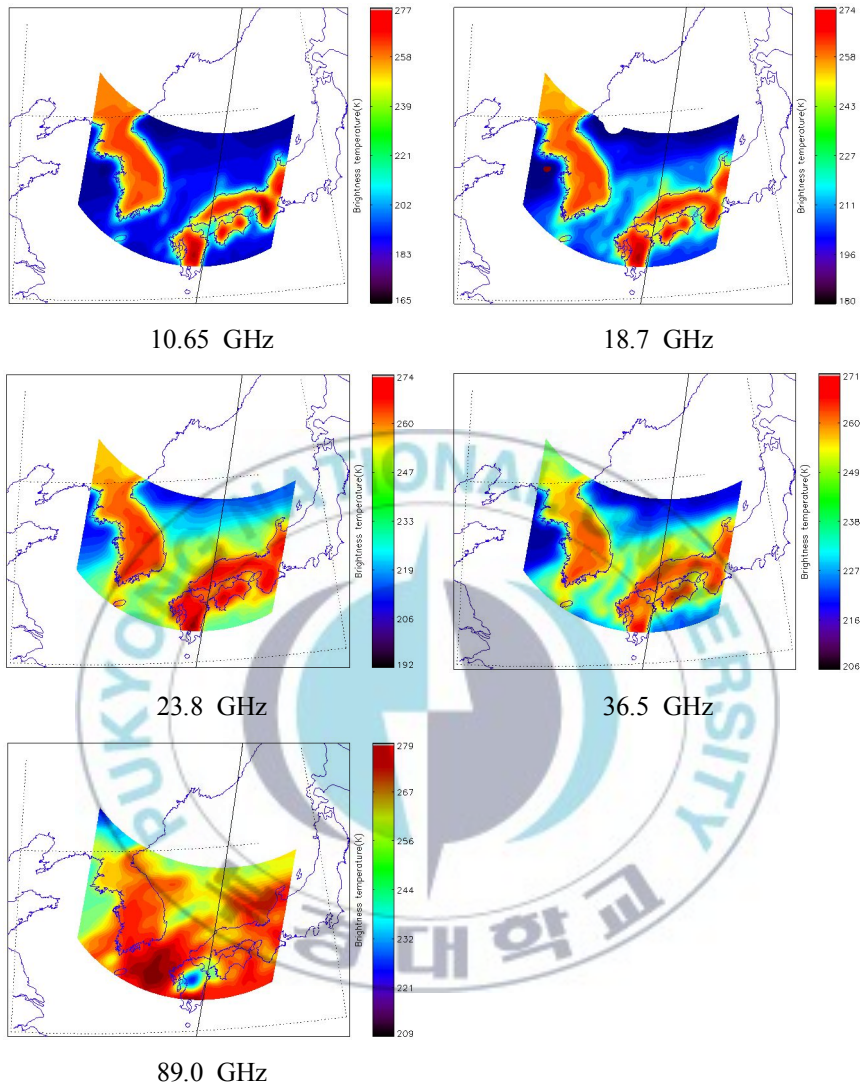


Figure 3.5. Images of CloudSat and AMSR-E channels on Feb. 3, 2008

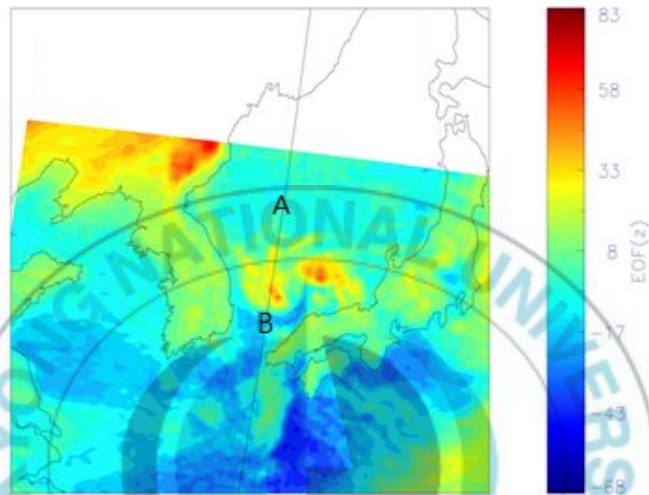
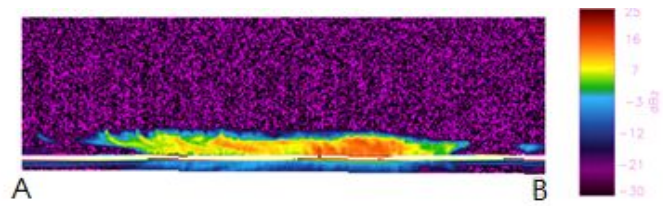


Figure 3.6. Snowfall cloud image comparison for instantaneous profile by CloudSat and horizontal distribution by CloudSat/MHS retrieval equation, February 3, 2008

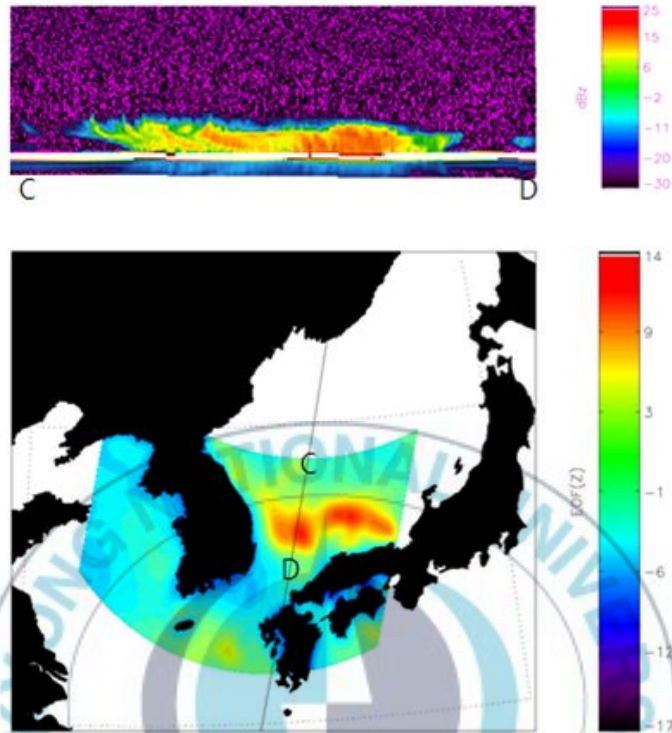


Figure 3.7. Snowfall cloud image comparison for instantaneous profile by CloudSat and horizontal distribution by CloudSat/AMSR-E retrieval equation, February 3, 2008

4. CONCLUSION

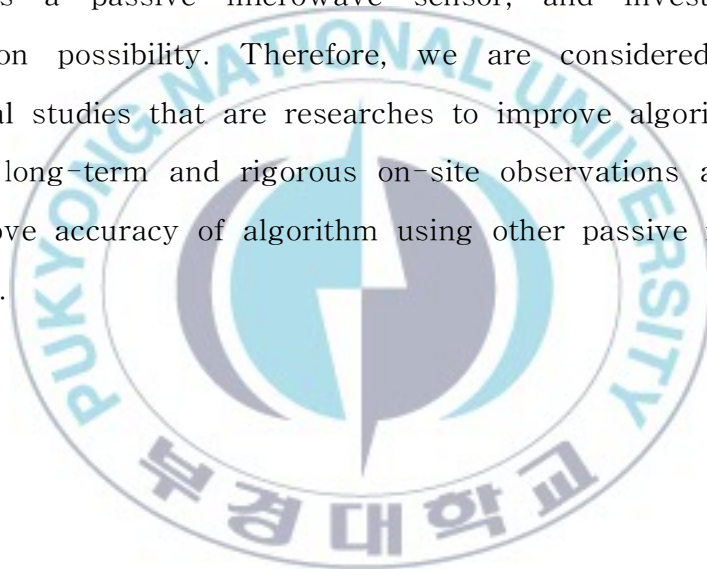
In this study, we developed snowfall retrieval algorithm by reflectivity of CloudSat-CPR and brightness temperature of AMSR-E and MHS. The principle components analysis was used to analyze the characteristics of snowfall, and linear regression equation was drawn by combining calculated values(Z' , w_i^T , k_i^T).

We investigated the relationship between Z' from CloudSat and combined algorithm in January and February, 2008. In case of MHS algorithm, correlation coefficient is 0.67 and 0.56, and RMSE is 2.27 and 1.92, respectively. In case of AMSR-E algorithm, correlation coefficient is 0.66 and 0.60, and RMSE is 2.67 and 2.36, respectively. Through the results, we confirmed observation possibility and applicability for snowfall from snowfall retrieval algorithm.

We performed the case study in Feb. 3, 2008, and were difficult to get snowfall signals through each of channels images. However, images applied algorithm was identified for snowfall signals at the East Sea area including Ulleundo, and existing snowfall in comparison with CloudSat reflectivity image. Then, algorithm by combining from MHS and CloudSat data shows a possibility of snowfall observation both ocean and land, but

algorithm by combining from AMSR-E and CloudSat data shows a observation possibility in only ocean area because of influence of land. Therefore, we are considered need to compensate the defect for algorithm.

In this study, snowfall retrieval algorithm was developed by combining reflectivity of CloudSat-CPR as an active microwave sensor and each of the brightness temperature of AMSR-E and MHS as a passive microwave sensor, and investigated an application possibility. Therefore, we are considered need to additional studies that are researches to improve algorithm using a more long-term and rigorous on-site observations as well as to improve accuracy of algorithm using other passive microwave products.



REFERENCES

- Annual Climatological Report, 2008. Korea Meteorological Administration, Seoul, Korea.
- Atlas, D., and O. W. Thiele, 1982. Precipitation measurements from space, Workshop Report, 5.4-5.9
- Choi, Y. J. and Shin, I. I., 1990. Statistical estimates of cloud thickness and precipitable water from GMS brightness data, Journal of the Korean Society of Remote Sensing, 6(2): 1-12
- Elena Lobl, Roy W. Spencer, Keiji Imaoka and Keizo Nakagawa, 2009. AMSR-E and its follow-on, AMSRw, Geoscience and Remote sensing symposium, 2009 IEEE International, IGARSS 2009: 77-80
- Gruber, A. 1973. Estimating rainfall in regions of active convection, J. Appl. Meteor., 12: 110-118
- Haddad, Z. S., and K. -W. Park, 2009. Vertical profiling of precipitation using passive microwave observation: The main impediment and a proposed solution, J. Geophys. Res.,

114, D06118, doi:10.1029/2008JD010744.

Kim, Y. S., Kim, N. R., and Park, K. W., 2011. Development of snowfall retrieval algorithm by combining measurements from CloudSat, AQUA and NOAA Satellites for the Korean Peninsula, *Korean Journal of Remote Sensing*, 27(3): 277-288

Kim, Y. S. and Park, K. W., 2002. Rainfall estimation using TRMM-PR/VIRS and GMS data, *Korean Journal of Remote Sensing*, 18(6): 319-326

Kongoli, C., P. Pellegrino, R. R. Ferraro, N. C. Grody, and H. Meng, A new snowfall detection algorithm over land using measurements from the Advanced Microwave Sounding Unit(AMSU), *Geophys. Res. Lett.*, 30(14), 1756, doi:10.1029/2003GL017177, 2003.

Lee, M. S., Kim, K. L., Suh, A. S., and Lee, H. H., 1994. Estimation of Precipitation Using Radar and Satellite Data, *Journal of the Atmospheric Sciences*, 30(4): 583-595

Level 2 GEOPROF product process description and interface control document algorithm version 5.3, 2007. A NASA

Earth System Science Pathfinder Mission

Limin Zhao and Fuzhong Weng, 2002. Retrieval of Ice Cloud Parameters Using the Advanced Microwave Sounding Unit, *J. Appl. Meteor.*, 41 : 384-395

Park, K. Y., 2000. Estimation of the realtime rainfall using TRMM and GMS data, The Graduate School, Pukyong National University.

Robinson, D.A., 1989. Evaluation of the collection, archiving, and publication of daily snow data in the United States, *Phys. Geogr.*, 10: 120-130

Sassen, K., and Z. Wang, 2008. Classifying clouds around the globe with the CloudSat radar: 1-year of results, *Geophys. Res. Lett.*, 35, L04805, doi:10.1029/2007GL032591

Schmidlin, T. W., 1993. Impacts of severe winter weather during December 1989 in the Lake Erie snowbelt, *J. Climate*, 6: 759-767

Seo, A. S., Lee, M. S., Kim, K. L. and Lee, H. H., 1994. An intercomparison of GMS image data and observed rainfall

data, Journal of the Korean Society of Remote Sensing,
10(1): 1-14



감사의 글

설레임과 두려움으로 시작했던 지난 2년간의 석사과정 생활을 돌이켜보면 힘든 시간들도 많았지만 많은 것을 경험하고 배울 수 있던 소중한 뜻깊은 시간이었습니다. 부족하지만 석사 학위 논문을 완성하기까지 격려와 칭찬을 아낌없이 주셨던 주위의 많은 분들께 진심으로 감사의 마음을 전하고자 합니다.

4년 전, 연구실에 처음 들어 왔을 때부터 석사 과정이 끝나는 지금까지 무한한 애정과 관심을 주신 김영섭 교수님께 마음 속 깊이 감사드립니다. 부족한 저에게 끊임없는 격려와 가르침을 주시고 제가 흔들릴 때마다 제자리로 돌아올 수 있게 많은 조언과 지도해주셔서 감사합니다. 그 동안의 말씀들 마음 속 깊이 새겨 더욱 더 발전하는 제가 되도록 노력하겠습니다.

학부생 때부터 많은 가르침과 관심을 주시고 석사 과정동안 많은 조언과 충고를 해주신 윤홍주 교수님, 배상훈 교수님, 최철웅 교수님, 서용철 교수님, 한경수 교수님, 그리고 이양원 교수님께 진심을 담아 감사의 말씀을 드립니다.

밤낮으로 제가 아프거나 힘들지 않을까 노심초사하시며 위로와 격려의 말씀을 아끼지 않으시고 늘 저를 위해 많은 기도 해주신 사랑하는 부모님과 군대에 있는 동안에도 누나 걱정 많이 해준 한술이, 아침저녁으로 고생이 많다며 한 말씀씩 해주시는 할머니께 진심으로 감사드립니다. 저를 아껴주는 부모님과 가족들 덕분에 무사히 석사 과정을 마칠 수 있었습니다.

미국에 계실 때부터 한국에 오신 지금까지 많은 가르침을 주신 박경원 박사님께 감사를 드립니다. 바쁘신 와중에 밤낮이 반대인 한국 시간에 맞춰 시간을 내어 주시고, 한국에 오셔서도 아낌없는 지도와 조언 해주셔서 늘 감사하고 죄송했습니다. 박사님 덕분에 많이 배우고 많이 성장할 수 있었습니다. 정말 감사합니다.

4년간 있었던 나의 연구실 가족들!! 내 연구실 생활의 대부분을 함께 했고 지금은 미국에서 열심히 공부하고 있는 진형이 언니. 머나먼 미국 땅에 가서도 늘 잊지 않고 큰 도움주고 내 푸념들 다 들어주어서 너무 고마워. 같은 연구실에서

생활하진 않았지만 그래도 우리방인 원석선배. 핀란드 가서도 잘 하시리라 믿어요. 같이 연구실 생활한지 1년이 채 안되지만 앞으로 같이 할 시간이 많은 돈정선배. 선배 덕분에 논문을 잘 마무리 할 수 있었어요. 정말 감사합니다. 앞으로도 잘 부탁드립니다!! 센터에 게시는 장재동 박사님과 기상청에 게시는 헤미언니께도 석사과정 동안 많은 격려해주셔서 감사하다고 전하고 싶습니다. 그리고 호주에 있을 의종이와 성규선배, 정훈선배, 경미언니에게도 늘 격려 해주셔서 감사하다는 말씀을 드립니다.

학부 1학년 때부터 석사 과정까지 늘 함께 해온 쾌활한 오지!! 졸업을 축하해. 내가 잘해주지 못해도 늘 내 생각해주서 너무 고마웠어. 때론 언니처럼 따끔한 충고도 아끼지 않았던 니가 함께 해줘서 힘들었던 석사 과정을 잘 마칠 수 있었어. 고맙고, 원하는 일들을 다 할 수 있길 바래, 화이팅!! 똑똑한 동생 하정이. 언니가 귀찮게 해도 웃으면서 다 받아주고 많은 도움줘서 너무 고마웠어. 넌 어딜가도 잘 할거라 믿어. 그리고 같이 석사 졸업하는 많은 동기 선배들. 다들 좋은 곳에 취직하길 진심으로 바랄게요.

석사과정 동안, 그리고 졸업하고 나서도 늘 격려해주고 힘이 되어 주는 인지 언니, 최지언니 너무 고마워요. 언니들이 저에게 많은 힘이 되었어요. 늘 나에게 파이팅 해주고 고민 상담해준 성희언니, 힘들 때마다 힘이 되어준 명환이, 꾸준히 안부전화 해주는 정년이, 힘들다하면 날 위해 큰 기도 해주는 양지, 맛있는 거 사주고 드라이브 시켜준 오빠들, 언니들, 항상 친절하게 IDL 가르쳐주신 광호선배, 학부 1학년 때부터 늘 변함없이 함께 해주는 하쭈와 가희, 그리고 먼 서울에서 나에게 무한 애정을 듬뿍 담아 보내주는 수희와 은주에게도 너무 고맙다고 전하고 싶습니다. 이 외에도 언급하지 못한 모든 분들께 진심으로 감사의 말씀을 드립니다.

늘 혼자라고 생각했지만 돌아켜보면 많은 사람들이 저에게 관심과 사랑을 주고 제 옆에 있어주었습니다. 미안하고 감사합니다. 받은 마음들 늘 잊지 않고 마음 속 깊이 간직하여 더욱 더 발전하도록 하겠습니다. 감사합니다.

2012년 1월
김나리 드림